Atmospheric water vapor continuum model for the sub-THz range

M.Yu. Tretyakov [a] [iD], T.A. Galanina [a], A.O. Koroleva [a],[*], D.S. Makarov [a], D.N. Chistikov [b],[c],
A.A. Finenko [a],[b],[c], A.A. Vigasin [a],[b]

[a] *Federal Research Center A.V. Gaponov-Grekhov Institute of Applied Physics, Russian Academy of Sciences, 46 Ulyanov Street, Nizhny Novgorod 603950, Russia*
[b] *A. M. Obukhov Institute of Atmospheric Physics, Russian Academy of Sciences, 3 Pyzhevsky Per., Moscow 119017, Russia*
[c] *Institute of Quantum Physics, Irkutsk National Research Technical University, 83 Lermontov str., Irkutsk, 664074, Russia*

ARTICLE INFO

ABSTRACT

Empirical and semi-empirical models of the continua absorption are still ubiquitously used in atmospheric science and applications despite almost a hundred-years-long persistent theoretical and experimental investigation of the continuum' nature. Based on the empirical knowledge accumulated to-date about the water vapor continuum we propose a physically sound continuum model for practical applications in the subterahertz frequency range (0-1 THz). Our model interpret the water vapor continuum in terms of a combination of various contributions owed to bimolecular absorption. The self-continuum component is presented in the model as a sum of the contributions from absorption by bound and quasibound dimers, which are evaluated with the help of the water vapor second virial coefficient and existing *ab initio* simulation of the water dimer absorption. The contribution from the far wings of the water monomer resonant lines is taken into account by virtue of a simple analytical function approximating available empirical data. The foreign-continuum component of absorption is taken in a conventional empirical form. The values of its numerical coefficients are updated to achieve better agreement with results of laboratory measurements in the sub-THz range. We demonstrate that our new model is in good agreement with modern versions of atmospheric propagation models. However, the atmospheric brightness temperature calculated using our new model systematically deviates from the results obtained with its empirical version. The deviation amounts up to several Kelvins in the microwindows between resonant water lines.

1. Introduction

Early attempts to describe absorption of radiation by the atmosphere solely in terms of line-by-line profiles of collisionally broadened lines of atmospheric molecules were made more than a century ago. Since then, no universally recognized theoretical description has been forged explaining how intermolecular interactions impact the atmospheric absorption giving rise to the so-called excess or continuum absorption. The observed excess absorption was initially interpreted as an unknown contribution by the far wings of intense resonance lines. This demanded including in the model an additional absorption that smoothly varies with frequency. It is referred to as the continuum absorption or just the continuum (see e.g. the reviews [1–4]). Significant progress has been achieved both in the theoretical interpreting the continuum as bimolecular absorption [5–7], and in practical recommendations for continuum modeling [8–10]. Nevertheless, the development of the continuum models is still based on empirical data obtained as the difference between the total observed absorption and the calculated sum of resonance lines. The value of empirically determined continuum is thus correlates with the data on line-shapes of the resonant absorption used to determine it. This makes difficult the comparison of continua values retrieved from different sources, not to mention the need to update the quantitative characteristics of the continuum when new sets of spectroscopic parameters for resonant spectra become available. The most complete semi-empirical description of the continuum in the entire frequency range significant for the Earth's radiation balance $(0–20,000 \text{ cm}^{-1})$ is represented by the Mlawer-Tobin_Clough-Kneizys-Davies (MT_CKD) model [11]. Complete description of all available data with this model is virtually impossible [12–14] since the continuum is modeled as the sum of contributions by the empirically modified far wings of resonance lines. This does not allow describing the spectra of double molecules (dimers), which can form in a gas from a couple of individual monomers. Although the number density of the water vapor dimers is small under atmospheric conditions, their role in absorption of

---

* Corresponding author.
  E-mail address: koral@ipfran.ru (A.O. Koroleva).

radiation can by no means be neglected. This was demonstrated both theoretically and experimentally (see [7] and references therein). The lack of a complete and accurate physically based model of all continuum components for atmospheric applications manifests itself in the systematic discrepancy between the results of two types of experimental data: (i) laboratory measurements under stable and well-controlled conditions, and (ii) field radiometric measurements under clear atmosphere conditions supported by radiosondes (Fig. 3 in [15] or Fig. 3.50 in [7]). For the same reason continuum uncertainty is the main factor limiting the accuracy of retrieving atmospheric parameters using the remote sensing techniques in the 24–45 GHz window of atmospheric transparency [16] and one of the most significant in higher frequency windows [17,18].

The goal of this work is to describe the water vapor related continuum based on the previously proposed physically grounded approach [9,19]. We expect to improve the accuracy of modeling the atmospheric absorption of radiation in the sub-THz frequency range actively mastered by modern methods of global satellite monitoring of the atmosphere [17,20]. Note that our approach enables, among other things, independent consideration of resonant absorption and continuum. As the prototype of the proposed model we use the complex refraction millimeter-wave propagation model (MPM), originally proposed by Hans Liebe [21]. This model was developed further by P.W. Rosenkranz [22,23] and usually denoted as PWR model. It is currently widely used for atmospheric applications in the considered frequency range and is more convenient for modifying continuum simulation in line with the goals of this work than MT_CKD.

Section 2 of this paper outlines the history of the PWR model development and the traditional method of continuum modeling. The proposed modification of the self- and foreign-continua in the PWR model is presented in Sections 3 and 4, respectively. In Section 5 we discuss potential uncertainties of the new model and verify its temperature dependences. Section 6 demonstrates the result of the model modification on the example of calculating brightness temperature spectra for downwelling thermal radiation in comparison with the initial model. The highlights and main results of our work are briefly summarized in the Conclusions.

2. The continuum in the PWR model

The original MPM model was proposed in 1978 in [21], where a procedure was presented for calculating the complex refraction of radiation at frequencies of 30–300 GHz during its propagation in the atmosphere. Later [24] the model was extended to frequencies up to 1000 GHz; however, its application for practical purposes was limited to the frequency region below 300 GHz, which is reflected in the name of the model given to it in 1983 [25]. The model includes the contributions of dry air (resonant absorption in atmospheric oxygen and the so-called "dry continuum"), water vapor, suspended water droplets (haze, fog, cloud), and rain. The input variables are pressure, temperature, relative humidity, suspended water droplet concentration, and precipitation rate. It is worth noting that the PWR model is still regularly updated as new, more accurate data on the related parameters become available [23].

Let us consider in more detail how the PWR model takes into account the absorption by atmospheric water vapor. The absorption is presented as the sum of profiles of the most intense H_2O lines (resonant absorption) and an empirically determined continuum, which is introduced to eliminate the discrepancy between the line-by-line sum and the observed absorption. Initially (in the model version of 1978), the resonant absorption was modeled as a sum of 6 lines in the 22–381 GHz frequency range with the Van Vleck-Weisskopf profile. The calculated contribution of the far wings from higher frequency lines (up to 31 THz) to the absorption in the considered range (30–300 GHz) was regarded to be the continuum. However, the observed continuum was not fully reproduced. The authors of the model noted that its main uncertainty is

related to the continuum absorption [21]. It is worth mentioning the advanced MPM version from 1989, where the resonance line list contained 30 lines up to 1 THz; their Van Vleck-Weisskopf profile wings were cut at the detuning from the center equal to 40 line widths; line shape parameters were taken from [26], and the continuum was empirically determined on the basis of extensive measurements at 138 GHz [27].

In the latest versions of the PWR model, resonant absorption is modeled as the sum of 19 strongest (integrated intensity $>10^{-25}$ cm/molec) H_2O lines in the region up to 1000 GHz. A list of line parameters is based on the HITRAN database [28] and is updated by the results of laboratory measurements, where possible. For a number of lines (for which measurement results are available) the influence of the collision cross-section dependence on the molecular speed ("wind effect") is taken into account. The model employs a resonant line profile based on the formalism suggested by Clough [29], which involves a wing cutoff at a detuning frequency of 750 GHz with the value of the line absorption at the cutoff frequency (sometimes called the 'pedestal' or 'plinth') subtracted from this line profile to avoid steps in the calculated absorption. Thus, the resonance line profile is reduced and pedestals under the lines are included in the continuum.

In the PWR model, the water vapor continuum absorption α_{cont}, including its linear C_f (foreign-continuum) and quadratic C_s (self-continuum) with partial water vapor pressure components is taken into account in the form of an empirical function, quadratically dependent on frequency, the same as in MPM89:

$$\alpha_{cont}(f, P, P_{air}, T) = C_s(f, P, T) + C_f(f, P, P_{air}, T)$$
$$= C_{s_0}\left(\frac{300}{T}\right)^{n_s} f^2 P^2 + C_{f_0}\left(\frac{300}{T}\right)^{n_f} f^2 P P_{air}, . \quad (1)$$

where f, P, P_{air}, T are, respectively, frequency (GHz), water vapor pressure (mbar), dry atmospheric air pressure (mbar) and temperature (K); C_{s_0} and C_{f_0} are numerical coefficients (in $cm^{-1}/GHz^2 mbar^2$) for the self- and foreign- continuum, respectively, n_s and n_f are their temperature exponents. The continuum absorption units are cm^{-1}. The results of the presented study will be compared with model (1) where the numerical coefficients C_{s_0} and C_{f_0} were determined in the work [30] as a result of the compilation of experimental data on the mm-wave continuum (138–239 GHz) known at that moment. Let us label the corresponding model version as the PWR98. The continuum parameterization in this model agrees very well with the results of thorough high-precision laboratory measurements in the mm-wave range (107–143 GHz) [31]. Nevertheless, in the later versions of the PWR model the continuum coefficients C_{s_0} and C_{f_0} were corrected for the sake of better agreement of the calculated brightness temperature with radiometric zenith measurements supported by radiosondes [32–34]. The current version (PWR23) employs the C_{s_0} value obtained as a result of approximation of the MT_CKD-4.1 continuum by function (1) in the region up to 1 THz.

No radiometric data was used to adjust the new model. For the further analysis we will use the continuum coefficients from the PWR98, namely $C_{s_0} = 1.8 \times 10^{-13}$ $cm^{-1}/GHz^2 mbar^2$, $n_s = 7.5$ and $C_{f_0} = 5.43 \times 10^{-13}$ $cm^{-1}/GHz^2 mbar^2$, $n_f = 3$, because they agree better with the laboratory experimental data obtained in well controlled conditions than the continuum coefficients obtained on the basis of radiometric measurements.

3. PWR-continuum upgrade

Analysis of the continuum spectra in the 0.45–1.5 THz frequency range [9,35,36] as well as the data obtained by Bohlander [37] in the 0.36–1.5 THz frequency range revealed that the frequency dependence of water vapor self-continuum differs noticeably from the quadratic function (1) in the sub-THz range. A similar conclusion follows from the difference (almost a factor of two) in the C_{s_0} continuum coefficients

obtained in the frequency ranges up to 0.1–0.3 THz [27,31,38,39] and above 0.7–2.4 THz [40] suggesting revision of the modeling approach. Both self- and foreign components of the continuum have the same collisional nature and, therefore, can be modelled using the same general approach, which is detailed in the next subsection on an example of pure water vapor continuum (self-component) simulation.

General approach to total absorption modeling

Under typical atmospheric conditions, water vapor can be considered as a mixture of H_2O molecules (monomers) with double molecules in pair states (stable and metastable dimers and free pairs) [5,41]. Therefore, the traditional subdivision of the total water vapor absorption $\alpha_{total}(f, T)$ into the sum of local/resonant monomer lines $\alpha_{local}(f, T)$ and continuum absorption $\alpha_{cont}(f, T)$ can be replaced by the sum of spectra of all water vapor components, namely spectra of monomers $\alpha_{mono}(f, T)$, stable (or true bound) dimers $\alpha_{BD}(f, T)$, metastable (or quasibound, hereinafter referred to as the metadimer for brievity) dimers $\alpha_{MD}(f, T)$, and free pairs $\alpha_{FP}(f, T)$.

The negligible role of radiation absorption by free pairs in water vapor under typical atmospheric conditions was demonstrated using rigid-rotor harmonic oscillator approach for the partitioning of pair states in [42,43]. Independent confirmation of this fact can be found in works [44,45]. Thus the $\alpha_{FP}(f, T)$ component can be safely omitted and the total absorption as usual is expressed as the sum of products of the number densities of the corresponding absorbers (n_m, n_{BD}, n_{MD}) by their normalized spectra

$$\alpha_{total}(f, T) = \widetilde{\alpha}_{local}(f, T)n_m + \widetilde{\alpha}_{cont}(f, T)n_m^2$$
$$= \widetilde{\alpha}_{mono}(f, T)n_m + \widetilde{\alpha}_{BD}(f, T)n_{BD} + \widetilde{\alpha}_{MD}(f, T)n_{MD}, \quad (2)$$

where the tilde symbol hereinafter denotes the absorption cross section of the corresponding absorbers. Following the far line wing modification approach first suggested in [29], we consider monomolecular absorption as the sum of reduced monomer line profiles $\alpha_{local}(f, T)$ with the 750-GHz cut-off from the line center and far wings absorption modelled as modified 'pedestal' under the lines $\alpha_{FW}(f, T)$. Analytical equations for
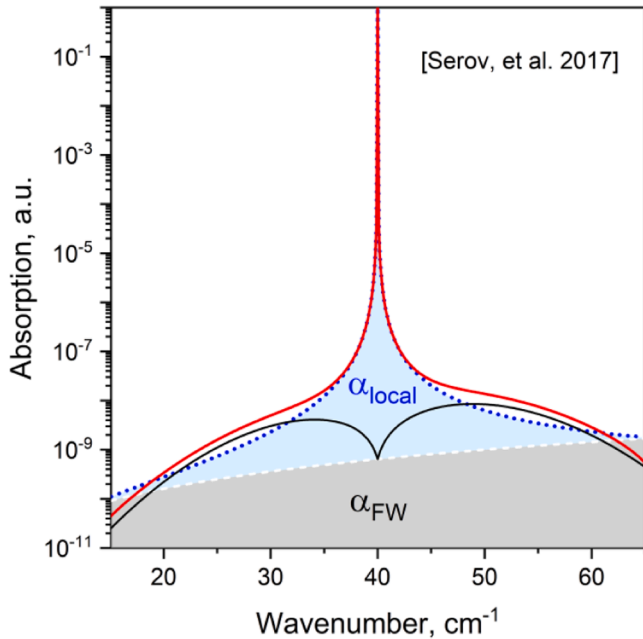
Fig. 1. Line wings approach. "True" line shape (red solid curve) obtained as the sum of the line shape in the impact approximation (blue dotted curve) and empirically modified pedestal under the line (black solid curve) obtained from the initial pedestal (gray area) by its multiplication by χ-function [19]. The blue shaded area corresponds to the traditional representation of local/-resonance line.

the wings modification given in [19] are used. An example of the line profile is shown in Fig. 1.

The figure demonstrates the difference between the line shape obtained within the impact approximation (dotted curve) and the gas-averaged spectrum of the evolution of the monomer dipole moment, including the time of interaction with the collision partner (red solid curve). Note super-lorentzian and sub-lorentzian behavior of the far wings at different detuning from the line center [19]. Let us consider the scaling of this far wing component $\alpha_{FW}(f, T)$ with monomer number density. It is well known that the growth of integrated intensity of a collision-broadened line with an increase in n_m is accompanied with the quadratic with n_m growth of the line wings amplitude rather than with the growth of the line amplitude at the line center [46]. Therefore, the monomolecular absorption normalized by n_m can be written as follows:

$$\widetilde{\alpha}_{mono}(f, T) = \widetilde{\alpha}_{local}(f, T) + \widetilde{\alpha}_{FW}(f, T)n_m \quad (3)$$

Note that details of this approach can be found in [9,19], where it was used for the interpreting the experimental data on $\alpha_{cont}(f, T)$ in the range of the H_2O fundamental vibrational and pure rotational bands. In the present paper we consider only what is important for practical modeling of the continuum.

Number density of dimers (including both bound and metastable dimes) can be found using the virial equation of the gas state, which can be safely truncated after the second term under atmospheric conditions:

$$P(n_m, T) = kT \cdot n_m + kT \cdot \frac{B(T)}{N_a} \cdot n_m^2. \quad (4)$$

Here N_a is Avogadro number and $B(T)$ is the second virial coefficient (SVC) related to pair intermolecular interactions in gas. Its value for water vapor is well established both experimentally and theoretically [47,48]. In this work we use the empirical data based approximation of $B(T)$ from [49], which is in a good agreement with *ab initio* calculations with full dimensional interaction potential [48]. Following [41], $B(T)$ can be subdivided into parts corresponding to the aforementioned bimolecular states: bound dimers $B_{BD}(T)$, metadimers $B_{MD}(T)$, and free molecular pairs $B_{FP}(T)$

$$B(T) = B_{BD}(T) + B_{MD}(T) + B_{FP}(T), \quad (5)$$

where

$$B_{BD}(T) + B_{MD}(T) = -K_D(T)RT, \quad (6)$$

R is the gas constant and K_D is the dimer equilibrium constant defined as

$$K_D = n_D / (n_m^2 kT) \quad (7)$$

and can be subdivided into bound and metastable dimer components:

$$K_D = K_{BD} + K_{MD} \text{ and } n_D = n_{BD} + n_{MD}, \quad (8)$$

$$B_{FP}(T) = b_0, \quad (9)$$

where b_0 is the so-called excluded volume. The limitations of the concept of the excluded volume were pointed out in many papers [41,43,50]. At very low temperatures it may even become negative thus having no literal meaning of any kind of excluded volume. As the first approximation one could neglect the contribution of excluded volume to the SVC of water vapor, because it definitely constitutes a small fraction of the total SVC at near room temperature. Not having known an exact value of $b_0(T)$, however, we are using hereafter its temperature independent value $b_0 = 30.5$ cm³/mole, which can be derived from the approximate van der Waals equation of state.

For the calculation of the bound dimers number density, we use empirical parameterization of the *ab initio* calculated values of $K_{BD}(T)$ (in atm⁻¹) from [51] corrected as described in [19] (Eq. (A7) in Appendix) using the dimer dissociation energy from [52]. It allows us to calculate the number density of metadimers n_{MD} using Eqs. (5)–(9) and

aforementioned parameterization of $B(T)$ (Eq. (A9) in Appendix)

A relative fraction of bound and metastable dimers in water vapor obtained by this way is shown in Fig. 2. Note a good agreement of the dependences with its estimation from [43].

Thus, summarizing Eqs. (2), (3), and (5) and assuming that $P = P_m$ (the partial pressure of dimers is small and can be neglected), the continuum absorption in water vapor can be written as

$$\alpha_{cont}(f, P, T) = \alpha_{BD}(f, P, T) + \alpha_{MD}(f, P, T) + \alpha_{FW}(f, P, T)$$
$$= C_{BD}(f, T)K_{BD}(T)P^2 + C_{MD}(f, T)K_{MD}(T)P^2 + C_{FW}(f, T)P^2, \quad (10)$$

where functions C can be considered as spectra normalized by partial pressure of corresponding absorbers.

Temperature dependence of the absorption was modeled assuming that each component of the continuum in the relatively narrow range of atmospheric temperatures follows a relevant power law:

$$\alpha_X(f, P, T) = S_X(f, T_0)\left(\frac{T_0}{T}\right)^{n_X} f^2 P^2, X = BD, MD, FW. \quad (11)$$

The term $S_X(f, T_0) = C_X(f, T_0)/f^2$ corresponds to the reduced spectral function (hereafter called just spectral function for simplicity) of bound dimers, metadimers and far wings, n_x are their temperature exponents. The f^2 term in (11) corresponds to the frequency dependence of the radiation term in the sub-THz range. The term is common for all types of absorbers.

In the next three subsections we report the results of our modeling of the frequency and temperature dependences of $S_X(f, T)$ spectral functions including determination of their temperature-independent part $S_X(f, T_0)$ and temperature exponents n_X.

Bound dimer absorption

The spectrum of a bound water dimer was modeled on the basis of thorough and the most accurate to date quantum chemistry calculations by Scribano and Leforestier [53]. Note that the calculated spectra (with the aforementioned D_0 correction applied) are in excellent detailed agreement with experimental observation of the dimer rotationally resolved spectrum in the mm-wave (0.1–0.26 THz) range [54–56] and with water vapor continuum study in the submm-wave (0.45–1.1 THz) range [9]. We decided not to reproduce in the model the rotational structure of the dimer spectrum mainly because the structure is effectively blurred under the influence of atmospheric pressure. The
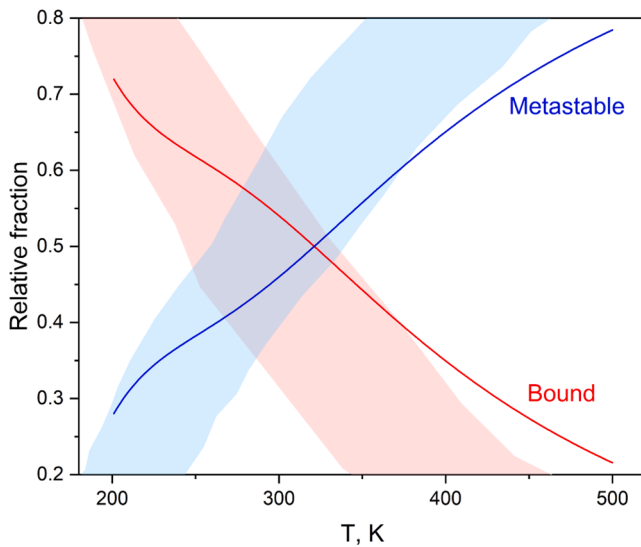
variation of the atmospheric brightness temperature corresponding to the structure at the vertical trace constitute about 0.1 K.

For the dimer spectrum modeling we used numerical data corresponding to the absorption spectra at 5 temperatures in the range of 268–308 K shown in Fig. 10 in [53]. A set of 4 temperature exponents was calculated using the neighboring pairs of these spectra:

$$n_{BD}(f) = \frac{ln(\alpha_{BD}(f, P, T)/\alpha_{BD}(f, P, T_0))}{ln(T_0/T)} \quad (12)$$

Then these data were approximated by a smooth function. The result is illustrated in the upper panel of Fig. 3. This function was used for recalculating the aforementioned five spectra of the dimer to 268 K (which is close to the mean temperature of the vertical atmospheric profile). The obtained numerical data were normalized by pressure and frequency squared and approximated using the following function:

$$S_{BD}(f, T_0) = \left(\frac{a_0}{(a_1)^2 + (f - a_2)^2} + \frac{a_3}{(a_4)^2 + (f)^2} + a_5\right). \quad (13)$$

Numerical parameters of the function are given in Table A2. For modeling the continuum we used Eq. (11) with this function and with the value of the exponent $n_{BD} = 10$ averaged over the frequency range. Note that, if necessary, the temperature and frequency dependence of the exponent can be easily taken into account (Fig. 3, upper panel. The high fluctuations below 100 GHz are due to numerical noise that occurs when small absorption calculated with a limited number of digits is normalized by f^2).

Metadimer absorption

A metadimer can be considered as some intermediate between a free molecular pair and a bound dimer [8,9,19,55,57,58]. Its effective spectrum is represented as a linear superposition of spectra of (i) two
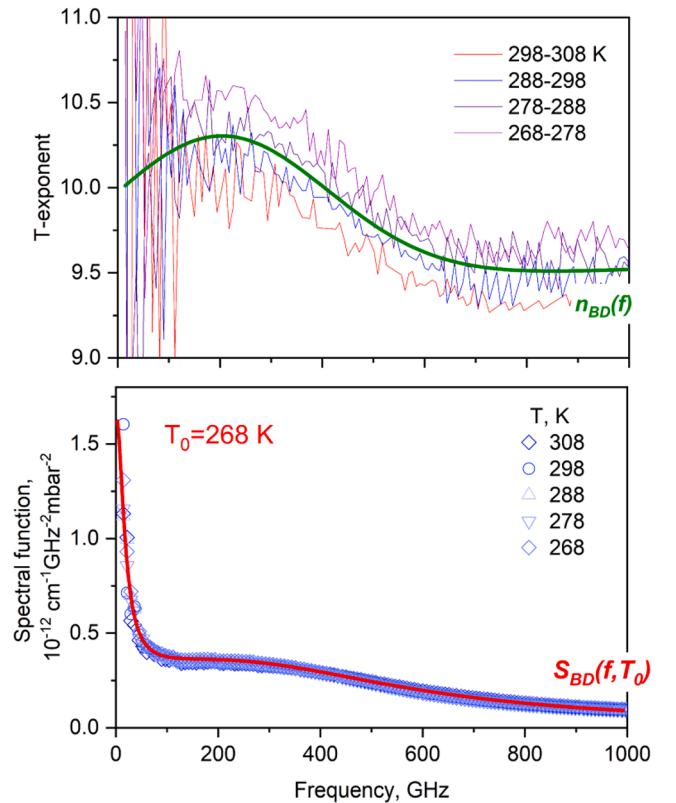

Fig. 2. Temperature dependence of relative fractions of bound (in red) and metastable (in blue) dimers corresponding to decomposition of water vapor SVC assuming $b_0 = 30.5$ cm^3/mol. Light blue and red areas are for estimations of the dependences from [43].

Fig. 3. Bound dimer spectrum [53] approximation. Upper panel: temperature exponent. Lower panel: spectral function data recalculated to 268 K (symbols) and their approximation by function (13).

monomers almost freely rotating next to each other and uniformly broadened by a short lifetime (the first extreme case) and (ii) a stable dimer (the second extreme case):

$$
\alpha_{MD}(f, P, T) = \left[S_{2mon}(f, T_0)\left(\frac{T_0}{T}\right)^{n_{MD_1}}(1 - N_D) \right.
$$
$$
\left. + \frac{S_{BD}(f, T_0)}{K_{BD}(T)}\left(\frac{T_0}{T}\right)^{n_{BD}} N_D \right] K_{MD}(T) f^2 P^2, \tag{14}
$$

where a N_D is an empirical parameter corresponding to the relative fraction of metadimers in the second extreme case. Note that this approach is qualitatively justified in the case of another bimolecular collisional systems CO_2-Ar [50] and N_2-N_2 [81].

The $S_{2mon}(f,T)$ spectral function was constructed using Van Vleck - Huber line shape [59] without wings cut-off, with the HITRAN2020 water line list in the 0–70 cm^{-1} range. The line width parameter was set to 12 cm^{-1} as a mean temperature-independent value obtained on the basis of the estimated metadimer lifetime of 0.3–0.8 ps [8]. The spectral functions were calculated for temperatures ranging from 206 up to 326 K (with a step of 10 K) in the frequency range up to 1 THz and their temperature exponents were evaluated using the same method as for the bound dimer spectral functions. The frequency dependence was approximated by a linear function. The result of recalculation of all spectral functions to 266 K using $n_{MD_1} = 2.9$ and their linear approximation is shown in Fig. 4.

Line wings absorption

The contribution of the water monomer resonance lines wing at large frequency detuning from the center is currently the most uncertain part of the continuum due to the lack of rigorous theoretical models and/or *ab initio* calculations [60]. Fortunately, as it will be shown below, this component is not dominating in the sub-THz continuum, especially at low temperatures. This component was taken into account on the basis of empirical information from [9], where water vapor continuum was interpreted in the range of H_2O rotational band (0.1–18 THz) at 296 and 326 K. A significant part of the continuum in this range, which cannot be attributed to molecular pairs, is considered as far wings of H_2O resonance lines using the semi-empirical model proposed in [19] and the list of H_2O lines from HITRAN [28]. The model employs two
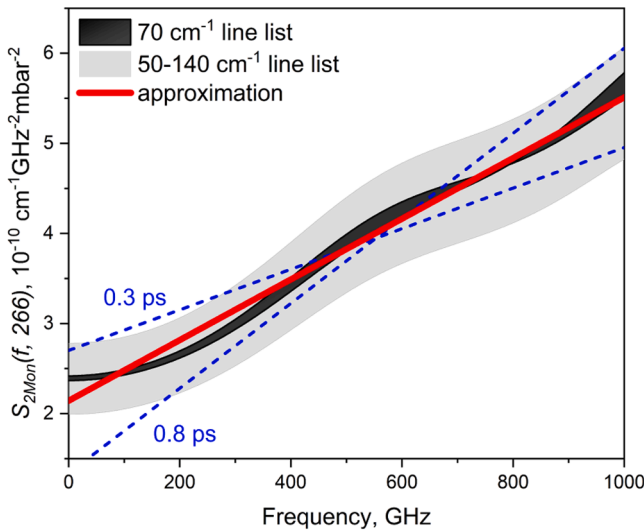
Fig. 4. Metadimer spectral function at 266 K as lifetime broadened and doubled spectrum of two monomers (thick black curve) calculated from 12 simulated water vapor spectra at temperatures ranging from 206 to 326 K. Red line is for the linear approximation of the spectral function. Gray area and dashed lines show uncertainty intervals of the function corresponding, respectively, to the choice of the highest frequency line in the list and to the dimer lifetime (see text for details).

variable parameters, A and $\Delta\nu$, characterizing the amplitude and the width of the super-Lorentz line shape component. Their values $A = 19$, $\Delta\nu = 15$ cm^{-1} for 296 K and $A = 14$, $\Delta\nu = 15$ cm^{-1} for 326 K were obtained in [9] based on the best agreement between the continuum model (10) and the available experimental data. A tempting option was just to use these data in the present model as is. However, it should be recalled that the model from [19] is *J*-independent (*J* is the total molecular angular momentum quantum number), although the underlying physics is based on molecular rotation during the collision time. The model provides satisfactory quantitative agreement with experimental data in the range of the H_2O rotational band maximum, where the imperfection of the model is averaged over many lines with a broad range of *J* values, but it cannot guarantee the same level of agreement at the edges of the band, where the contributions from concrete *J*-lines are significant. Keeping this in mind it was decided to approximate the far wing component in the new model by a simplified empirical function:

$$
S_{FW}(f, T) = c \cdot f^{ns} \cdot \left(\frac{T_0}{T}\right)^{n_{FW}} \cdot P^2, \tag{15}
$$

where c and ns are variable parameters of the model. The unknown value of the temperature exponent n_{FW} was adopted from continuum temperature dependence measurements in the H_2O rotational band (Fig. 3 in [61]). The dependence is stipulated by two mechanisms (H_2O dimers and far wings) acting simultaneously. It reaches a minimum ($n \sim 1.5$) at about 300–500 cm^{-1}, which means that n_{FW} cannot be larger than 1.5. At the same time, Fig. 2 in [9] shows that the far wing component is dominating in this range; therefore n_{FW} cannot be much smaller than 1.5. In the absence of any other information, the value is fixed at 1.5. Note that the values of c and ns were determined by fitting the entire model to the experimental data in the sub-THz range as described in the next section. The empirical data on the far line wing continuum component from [9] were not used in the fitting procedure. Fig. 5 demonstrates that these data obtained at 326 and 296 K and 16 mbar are in reasonable agreement with our model predictions.

Self-continuum model fitting to the experimental data

Finally, our H_2O self-continuum model Eq. (10) has only 3 fitting parameters: the far wings component amplitude c, the frequency dependence exponent ns, and the relative number of two different types of the metastable dimer N_D. These parameters were fitted to two sets of the most accurate laboratory experimental data in the sub-THz range: (i) a rigorous study of the continuum in the 107–143 GHz range with the double resonator technique [31] in a broad range of atmospheric pressures and temperatures, and (ii) a broadband study of the continuum in the 400–1500 GHz range at room temperature using FTS with SOLEIL synchrotron radiation source [36]. Note that for consistent analysis all the used experimental continuum data were corrected, when necessary, to achieve the universal approach of taking into account the resonant absorption calculation used for continuum retrieval, namely, including or neglecting the pedestal under the line in the continuum.

Fig. 6 demonstrates the result of this fitting corresponding to the following parameter values: $c = 7 \times 10^{-15}$ $cM^{-1}GHz^{-2.2}mbar^{-2}$, $ns = 2.2$, and $N_D = 0.7$. Note that the experimental data used for the model fitting are in a good agreement with results of many other well-known laboratory studies of the continuum in the mm and submm wave range, and well supported by the field measurements data with a long optical path along the surface [39]. The interested reader is addressed to Fig. 3 in [15] or Fig. 3.50 in [7], where all of these data are plotted together.

Fig. 7 shows how the new model corresponds to some of these other data and allows comparing the model with its predecessor PWR98 and with the most recent MT_CKD-4.3 model [62]. In the frequency range up to about 0.4 THz, all the models agree well with each other and with experimental data. This is explained by the fact that their numerical coefficients are fitted to the same empirical data. At higher frequencies the proposed model reproduces experimental data from [36,37,40] significantly better than the PWR98 and MT_CKD models.
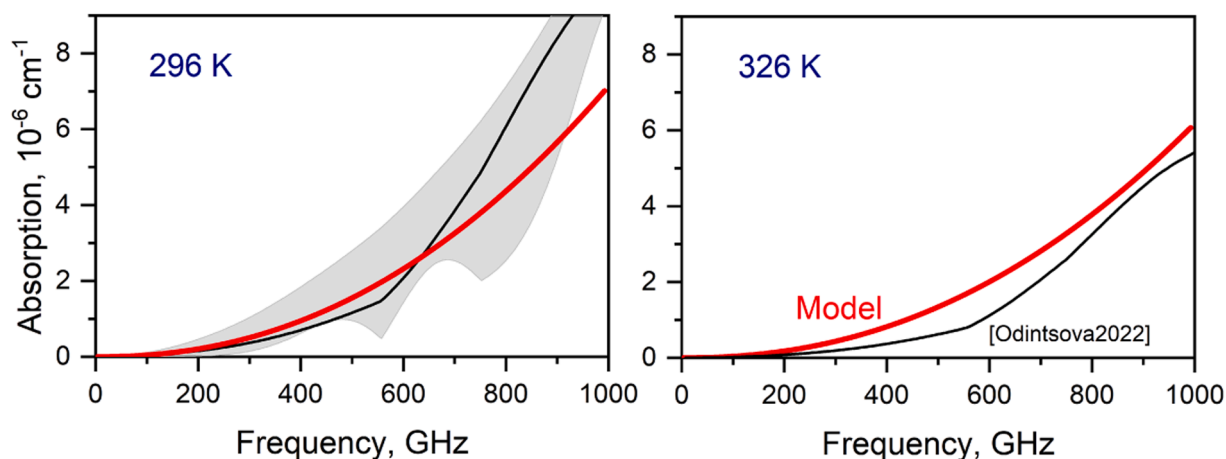
Fig. 5. Contribution of far wings of H_2O lines to the absorption coefficient of water vapor at 296 K and 326 K, 16 mbar: as empirically determined in [9] (black) and as obtained from the new model Eq. (15) (red). Gray area in the left panel is estimated uncertainty range for the black curve on the basis of data from [36].
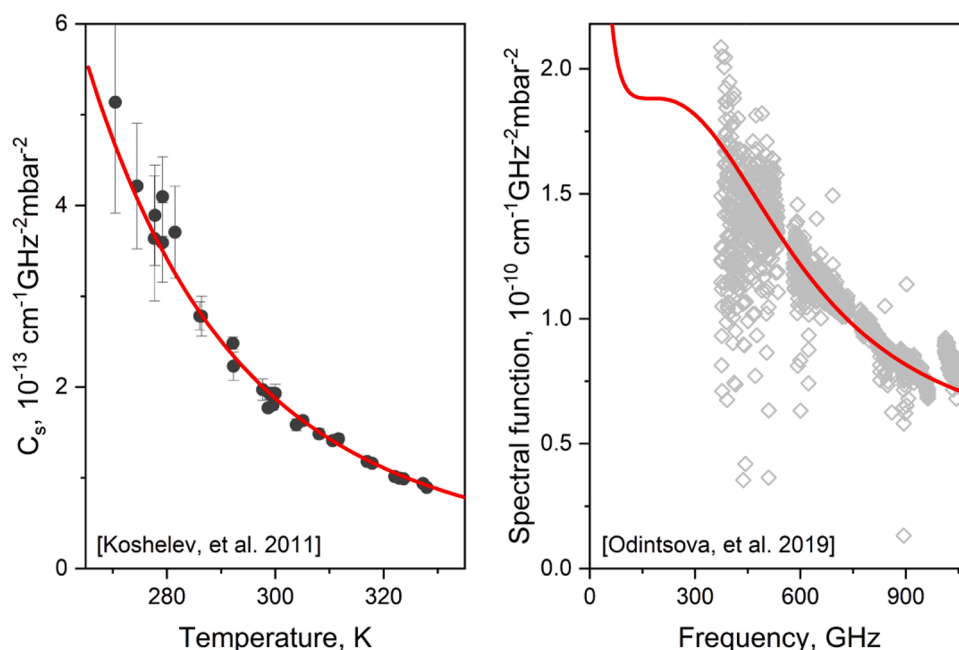

Fig. 6. Result of fitting the self-continuum model (solid line) to experimental data (points) in the mm wavelength range from [31] and in the submm range from [36].

The subdivision of the modeled self-continuum into its three components (Eq. (9)) at three typical atmospheric temperatures 260, 290 and 320 K is shown in Fig. 8. Note a significant deviation from the PWR98 at low temperatures and high frequencies.

Foreign-continuum upgrade

Physically based modeling of a foreign component of the humidity-related atmospheric continuum is impossible because of the lack of reliable theoretical calculations of bimolecular absorption in H_2O-N_2 and H_2O-O_2 collisional systems. However, we believe that the modeling accuracy of the component in a broad mm-submm wavelength range can be also improved by fitting the coefficients of the corresponding part of the empirical Eq. (1) to available experimental data. Recall that in the PWR98 these coefficients were determined on the basis of the mm wave range data only. Their agreement with the model can be found in Fig. 3 in Brognies et al. [15] or Fig. 3.50 in [7]. Note that the PWR98 adopted temperature exponent $n_f = 3$, corresponding entirely to T-dependence of the radiation term following the results of laboratory study by Liebe [27], although subsequent measurements by Bauer's group [63–65] and

by Koshelev et al. [31] indicated somewhat stronger T-dependence. In addition to these data, the foreign-continuum parameters in the submm range were obtained by Pardo et al. under unique El-Nino conditions at 272 K [67] and by Podobedov et al. at 293–333 K [40,66]. The quadratic frequency dependence of the continuum was assumed in all aforementioned studies, although the spectral functions of H_2O—N_2 and H_2O—O_2 bimolecular systems are also expected to have a broad maximum at low frequencies and decreasing behavior in the submm range as H_2O—H_2O spectra (Fig. 6 right panel). Keeping this in mind, we use the frequency dependence exponent as an additional variable parameter of the model. The best agreement of the model and the aforementioned experimental data was obtained at the frequency dependence exponent equal to 1.96, $C_{f_0} = 7.1 \times 10^{-15}$ cm^{-1}/GHz^{2}mbar^2 and $n_f = 4.4$. Fig. 9 illustrates the agreement between the model and the data from [31]. These data were recalculated from H_2O—N_2 to H_2O-air continuum using the efficiency factor 1.124 from [27], which was found in a good agreement with the efficiency factors determined using the experimental data from [40,66].

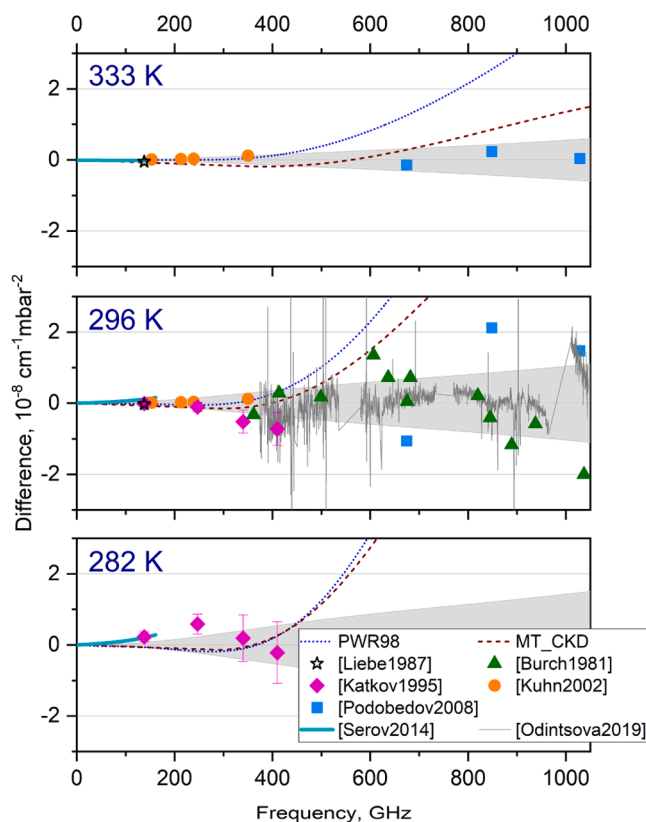All other data are compared with the new model, with PWR98, and

Fig. 7. Deviation of PWR98, MT_CKD-4.3 and experimental data on the self-continuum from the new model at 282 K, 296 K and 333 K. Estimated uncertainty of the model is shown by gray area.

with MT_CKD-4.3 in Fig. 10. Note very close agreement of the new model with MT_CKD and notable deviation from PWR98, especially in the sub-THz range.

4. Discussion

Uncertainty sources of the model

We emphasize that, despite the incomplete theoretical information about the H_2O-related bimolecular absorption, our self-continuum absorption model has only three fitting parameters. Two of them (*ns* and *c*) are responsible for the most uncertain far wings component of the continuum. The magnitude of the uncertainty can be evaluated using data of Fig. 11 in [36], where it is demonstrated that satisfactory agreement between the experimental continuum at 296 K and its simulation can be obtained within a broad range of parameters of the far wings model [19]. The impact of the far wings variation from one extreme case to another is shown in Fig. 5 by gray area. It can be seen that in the considered sub-THz frequency range the uncertainty interval is close to the variation of the far wings component of the continuum within 296–316 K. We believe that one of the most promising ways to develop a *J*-dependent model for far wings of resonance lines is the method of semi-classical trajectories, since it enables detailed monitoring of the evolution of the dipole moment of a monomer during collision [68].

The third fitting parameter N_D of our self-continuum model characterizes the effective spectrum of metadimer. This spectrum should be understood in terms of the average spectrum characterizing the ensemble of quasibound dimers, the life-time of each of which may differ by orders of magnitude. General applicability of such an approach for H_2O-H_2O metadimer spectrum modeling is supported by similar simulation for the CO_2-Ar [50] and N_2-N_2 [81] systems, for which all the required spectra were calculated using the classical trajectory-based

simulation method. Our calculations indicate that, within a broad range of temperatures (200–300 K) all the features of the metadimer spectrum can be sufficiently well reproduced by a linear superposition of the bound dimers and free pairs spectra and the coefficients of the superposition can be considered to be temperature independent. For the H_2O-H_2O dimer, the parameter N_D was found to be anticorrelated with the parameter *c* from the far line wings model. Consequently, the aforementioned uncertainty of the far wings extends to the metadimer model. The same uncertainty characterizes the metadimer model when the two monomer spectrum $S_{2mon}(f,T)$ is considered in terms of the metadimer effective spectrum, through the choice of the number of lines to be considered. Indeed the process of the dimer dissociation into monomers is not instant; therefore, the line wing is not Lorentzian and the frequency at which the line list should be cut is uncertain. To estimate the impact of this uncertainty we varied the highest frequency in the list of monomer lines from 50 up to 140 cm^{-1}. The corresponding deviation of spectral function magnitude constituted about 9 % (gray area in Fig. 4), which was compensated in the model by the same variation of N_D parameter. The uncertainty of the metadimer lifetime estimation (dashed blue lines in Fig. 4) has a similar impact on the model. Note that the N_D value is rather well fixed within the interval 0.65–0.75 by the temperature dependence of the self-continuum in the mm range and the frequency dependence of the continuum in the submm range (Fig. 6). This part of the continuum model can be also improved by explicit calculations of the H_2O-H_2O metadimers spectrum using the classical trajectory-based simulation as for CO_2-Ar [50,69,70].

Recall that the bound dimer absorption is simulated on the basis of *ab initio* calculations from [53] and has no variable parameters in our model; however, uncertainty of this component should be also addressed. The most prominent disadvantage of these calculations is the use of imperfect potential energy surface (PES). Our correction of the D_0 value does not mitigate significantly potential inaccuracies of the calculated partition sum and wave functions (especially for thermally populated highly exited vibrational states of the dimer) influencing line intensities and, therefore, the shape of the spectrum. The only way to improve the model is to repeat the calculations using the advanced full-dimensional PES from [71].

The next source of uncertainty of the self-continuum components is water vapor SVC. The parametrization of SVC used in this work [72] is based on empirical data. Its deviation from the results of quantum chemical calculations with the full-dimensional PES from [71] can be estimated using the data plotted in Fig. 1 in [73]. Their analysis suggests, that in the range of warm atmospheric temperatures (above freezing), the deviation does not exceed 7 %. The authors of the potential believe that such an agreement "assesses the very high quality of the global potential" [73], thus the uncertainty of the empirical data in this *T*-range is presumably much higher. Below freezing, the parametrization of empirical information becomes an extrapolation and at 250 K the uncertainty of SVC can be roughly estimated to be about 20 %. Fortunately, the impact of this uncertainty on the total calculated atmospheric absorption is not very significant because the water vapor content in air decreases fast with temperature decrease.

Note that all aforementioned uncertainty sources influence the accuracy of absorption predicted by the model only beyond the range of available experimental data, which were used for the model fitting. It is not easy to evaluate the uncertainty of the model in the range of the parameters, where it extrapolates experimental data. However, this uncertainty should be definitely smaller than the uncertainty of the empirical model (1) because of the used physically grounded approach. The major model uncertainty factor is the uncertainty of experimental data. The latter consists of statistical uncertainty (given by the amount and spread of measured data) and potential systematic error (related to the ambiguity of the resonance absorption subtraction). In our case, the statistical uncertainty of experimental data [31] (107–143 GHz, 260–330 K) is about ±10 % for both the self- and foreign-continuum components. Empirical approximation of the total absorption (without
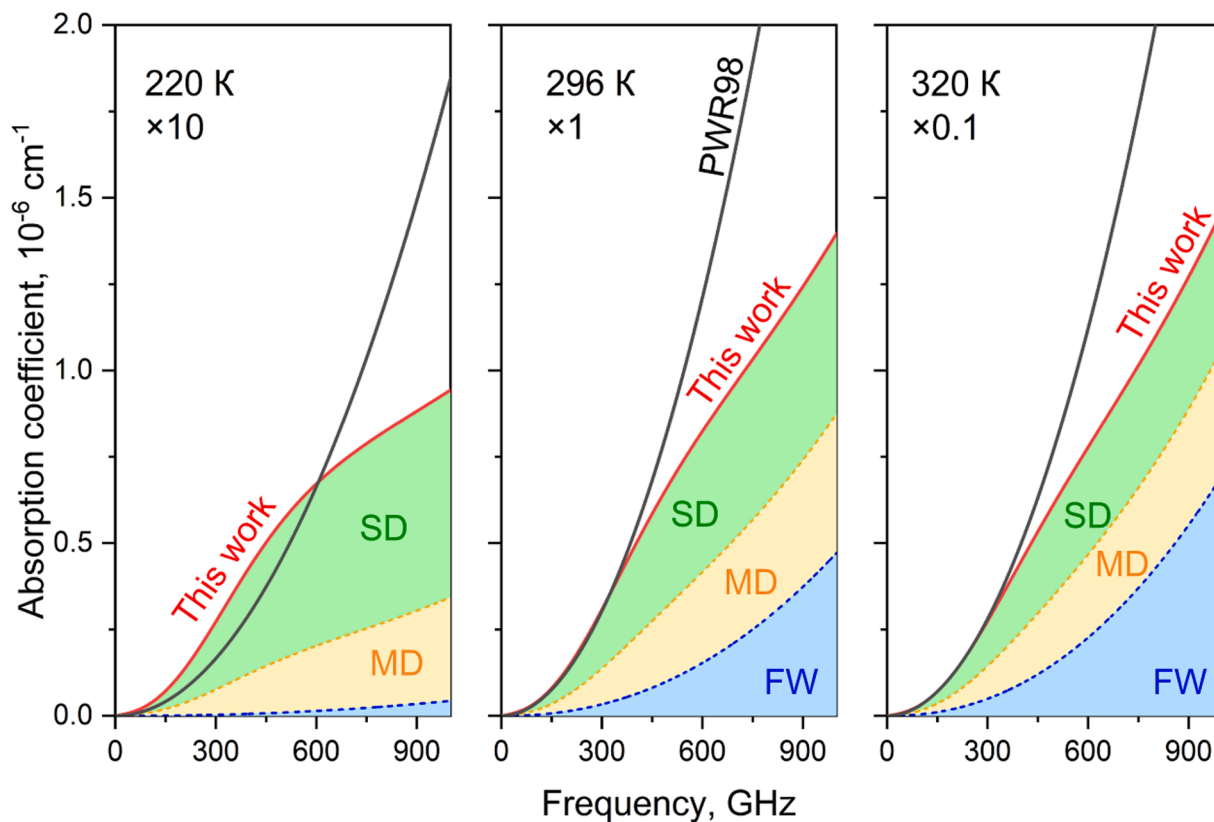
Fig. 8. Components of the continuum spectrum at 220, 296 and 320 K and, respectively, 1, 13 and 53 mbar of water vapor pressure corresponding to far line wins (blue area), metastable (yellow) and bound dimers (green). The total simulated absorption is shown by red solid line. Note the vertical scale multiplier, which is different for each panel. Absorption calculated by PWR98 is shown by black solid curve.
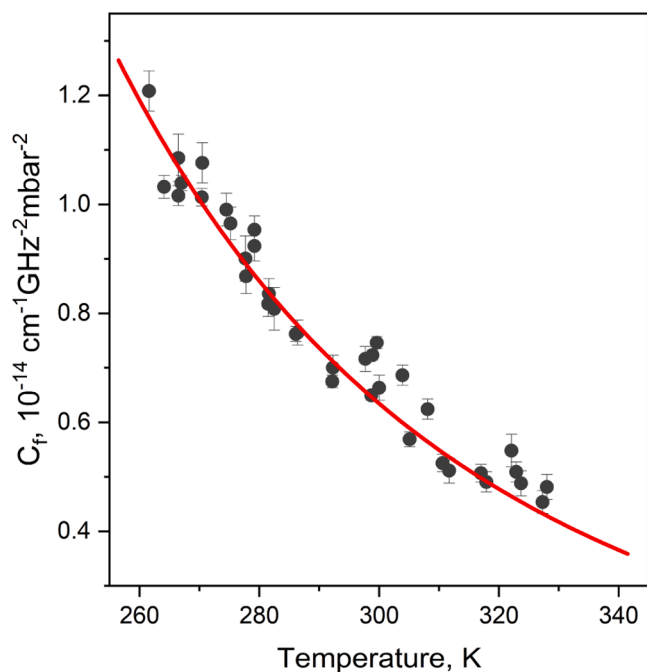
Fig. 9. Comparison of the new model (solid curve) with foreign-continuum measurements by Koshelev et al. (dots) [31].

resonance spectrum subtraction) was described in [31]. It allows evaluating potential systematic uncertainty of these data by using a different set of resonant line parameters. Such estimates show that systematic
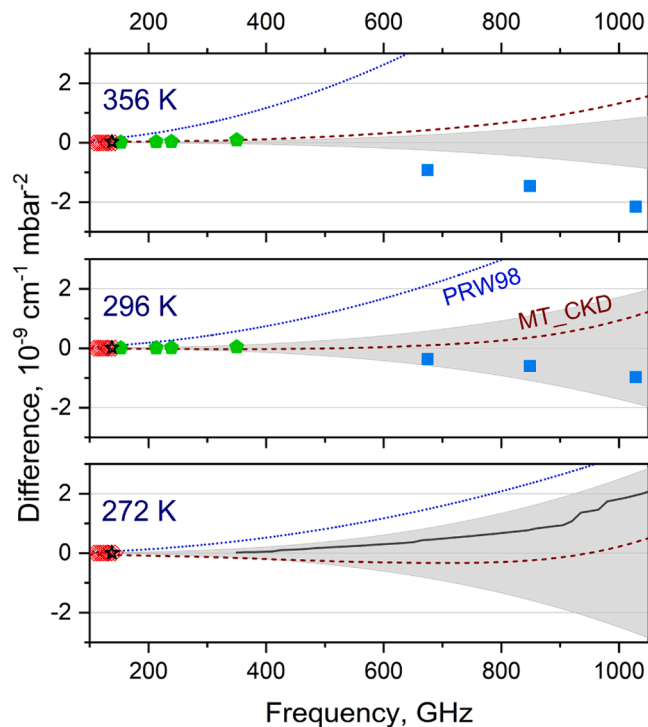
Fig. 10. Deviation of PWR98 (red dashed curve), MT_CKD-4.3 (blue dotted curve) and experimental data ([31] – red rhombs, [38] – green pentagons, [40] – blue squares and [67] - solid black curve at 272 K) from the new foreign-continuum model at 272, 296 and 356 K. Estimated uncertainty of the model is shown by gray area.

variation of the retrieved continuum coefficients is <5 %. The experimental data from [36] (300–1050 GHz, 296 K) have statistical uncertainty of about 7 % and potential systematic error of about 3 %. These estimates allow suggesting that the total uncertainty of the self-continuum model at room temperature is <12 % within the considered sub-THz frequency range. The same uncertainty is expected for the self-continuum at temperatures within 260–330 K in the frequency range below 200 GHz. For the foreign-continuum the uncertainty is about the same below 200 GHz but it gradually grows with frequency up to about 25–30 % at 1 THz due to significant systematic difference between two (seemingly equally reliable) datasets from [40] and [67]. One more foreign-continuum dataset is available from [74]. Review of these data reveals following problems: (i) the resonance line list includes only 7 strongest water lines, which are modeled with the Van Vleck – Weisskopf profile without wings cut-off and (ii) the self-continuum is modeled using Eq. (1), which is not valid for the broad frequency range, and with C_f value obtained in [40] using a different approach for the resonant spectrum subtraction. Thus, these data cannot be used either for fitting the model or for its uncertainty evaluation before proper re-treatment.

Temperature dependences

Verification of the absorption temperature dependence can be a validation test of the model. A general approach to assessing the expected *T*-dependence of bimolecular absorption is outlined in detail in [75,76]. The approach is based on the law of equipartition of kinetic energy among all its various forms including, in particular, translational, rotational and vibrational motion. The partitioning depends on the properties of intermolecular interaction potential and on the number of degrees of freedom of individual monomers and the molecular complex they can form in the collision. Consideration of these features allows to derive a very general estimate for the expected *T*-dependence of absorption in gases and their mixtures:

$$C_{X-Y}(f, T) = C_{X-Y}(f, T_0) T^n \left(exp\left(\frac{D_0}{k_B T}\right) - \left(1 + \frac{D_0}{k_B T}\right)\right), \quad (16)$$

where D_0 – is the dissociation energy of a molecular complex *X–Y*, $n = 7/2 - m$ (for the sub-THz continua, where radiation quantum energy is much smaller than thermal energy), and *m* acquires intermediate values between m_{min} and m_{max} which are fixed by the rotational and vibrational degrees of freedom of the complex and the parent molecules-monomers (see Table 1 in [76]).

For the self-continuum component of our model (Eq. (10), excluding the $S_{FW}(f,T)$ term), we take $D_0 = 1108$ cm^{-1} [52], $m_{min} = -0.5$, $m_{max} = 2$ and, therefore, the expected *n* value ranges within 1.5 – 4. The *n* value retrieved from our model was found to be frequency and temperature dependent, well within expected interval (Fig. 11). Moreover, the

obtained $n(f,T)$ dependences are in a good agreement with theoretical predictions. The general trend of the curves reflect the fact that a colder dimer has fewer rotational degrees of freedom, and, therefore, a smaller *n* value. The slope of the curves decreasing with frequency reflects the decrease of the bound dimer spectral function with frequency increase (Fig. 3, upper panel) and the decrease of its dominating role in the self-continuum.

For the foreign continuum component such evaluation is complicated by the composition of air. The continuum is basically a superposition of two components corresponding to atmospheric oxygen and nitrogen; the experiments [27,66] showed that the O$_2$-component is much smaller than the N$_2$-component but not negligible. However, both collisional systems H$_2$O-N$_2$ and H$_2$O—O$_2$ are similar in terms of the interaction potential (D_0 is about 105 and 67 cm^{-1} for N$_2$ and O$_2$, respectively [77]) and have the same number of degrees of freedom ($m_{min} = -0.5$, $m_{max} = 1.5$, expected *n* interval from 2 to 4). Thus, for the qualitative estimation we can assume that *T*-dependence of the foreign continuum is governed by H$_2$O-N$_2$ collisions. The value of *n* retrieved from our model also agrees with the prediction as shown in Fig. 11, right panel.

The sensitivity of this *T*-variation test to small changes of the foreign continuum *T*-exponent can be demonstrated on an example of PWR98, where $n_s = 7.5$ and $n_f = 3$. Recalculation of the model *T*-exponents using Eq. (16) gives *n* ranging from 0.62 to 2.2 for the self-continuum and the constant value of 0.76 for the foreign continuum (Fig. 11, dashed curves). These values are outside the expected interval: partly for the self-continuum (below freezing) and completely for the foreign continuum (at all temperatures). Most demonstrative is the case of the foreign continuum which shows that a minor change (within triple statistical error of experimental data from [31]) in the model exponent violates the agreement with theoretical expectation.

5. Brightness temperature

In this section we examine the impact of the proposed changes to the PWR model on the calculation of the brightness temperature (T_b) of the Earth's atmosphere as measured by a radiometer. To simulate brightness temperature we used the PyRTlib library [78] built on the basis of a code for similar calculations [22]. This library allows simulating the brightness temperature of the atmosphere in the frequency region up to 1 THz, measured by ground-based (downwelling T_b) or satellite radiometers (upwelling T_b).

As an example, we present the simulation of the downwelling T_b in the 0.1–1 THz range, measured with a radiometer located at an altitude of 5 km above sea level. A standard tropical profile from the PyRTlib library was used. Recall that the most significant contribution to the absorption of electromagnetic waves by atmospheric air is determined
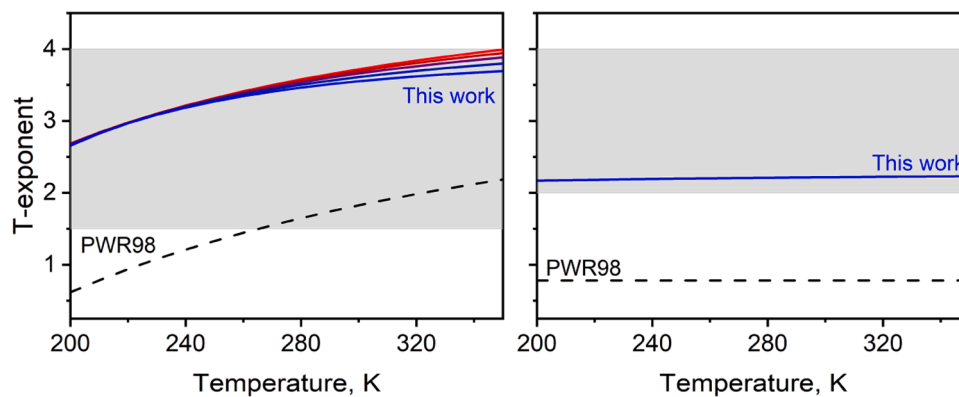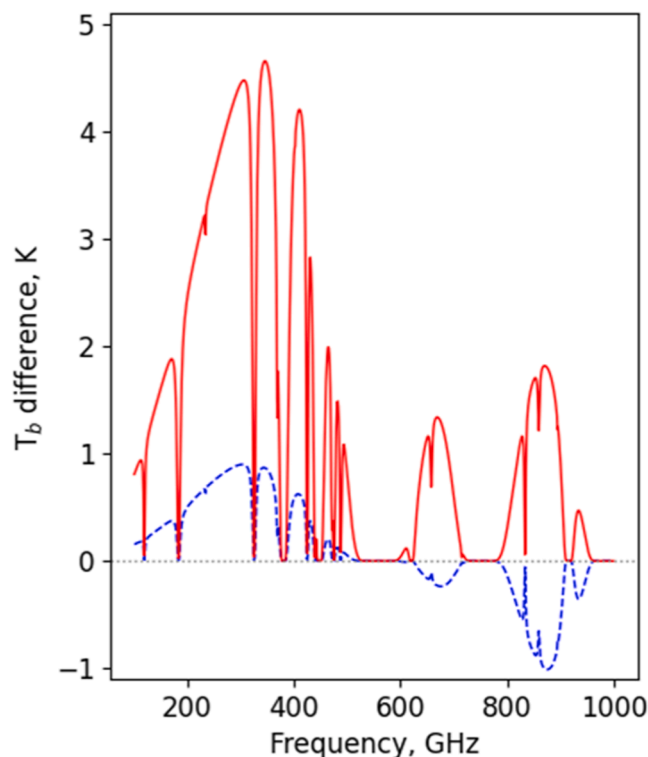

Fig. 11. Temperature exponent of the self- (left) and foreign (right) continuum components as follows from Eq. (16). The exponents (solid curves) are calculated for the new model at 100, 500, 700, 900 and 1100 GHz (colors vary from red to blue). The corresponding dependences for PWR98 are shown by dashed lines. Grey areas are the theoretically expected exponent ranges.
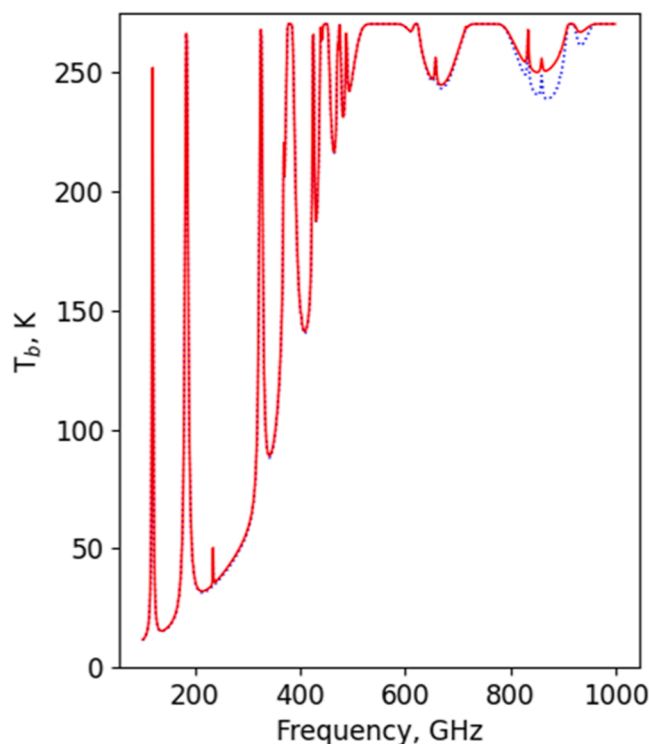
Fig. 12. The difference between the calculated brightness temperature corresponding to zenith measurements from an altitude of 5 km from sea level using the proposed continuum absorption model and PWR22 (see text for details).

Fig. 13. Estimated atmospheric brightness temperature corresponding to zenith measurements from an altitude of 5 km from sea level using a list of resonance lines up to 1 THz (blue dotted curve) and the same list extended to 1.75 THz (red curve).

by the resonant absorption (i.e., spectral lines of atmospheric molecules), which is summed with the continuum absorption. Correct comparison of different continuum models requires application of the same approach to spectral lines modeling. Fig. 12 shows the difference between the brightness temperature calculated using the proposed water vapor continuum absorption model and the empirical continuum model PyRTlib/PWR22, both using the same resonance spectrum line list and line shape parameters from PyRTlib/PWR22. (However, even in this case we neglect the aforementioned potential systematic difference related to the current necessity of employing the continuum model together with the same line list, which was used for the continuum retrieval.) The difference in the calculated brightness temperatures reaches about 1 K at frequencies near 350 GHz and about –0.8 K near 900 GHz if only the self-continuum component is replaced and up to 4.7 K if both the self and foreign components are replaced with the new model.

Note that the selected conditions for comparison are the most favorable for the new model and probably demonstrate a maximal, rather than a typical deviation from the currently used models. For example, a similar comparison for the satellite nadir observation (up-welling radiation) gives a maximal difference of about 0.5 K and 0.9 K for the self- and for both continuum components, respectively.

It is worth noting that the PyRTLib library uses a list of water molecule lines with frequencies up to 1 THz. Since the line profile corresponding to resonant absorption is cut off at an offset frequency of 750 GHz from the line center, to adequately simulate the absorption spectrum and brightness temperature in the region up to 1 THz it is necessary to extend the line list to 1.75 THz. The difference between the brightness temperature calculated using the line list from the current PWR23 version and the list extended to 1.75 THz based on HITRAN data is 20–30 K in transparency microwindows near 1 THz, exceeding the difference due to the use of different continuum absorption models by about an order of magnitude (Fig. 13). This consideration demonstrates a crucial importance of careful allowance for all factors influencing the

continuum for physically based modeling.

6. Conclusion

The comparison of known experimental data on the water vapor continuum and the simplest empirical function from the MPM89/PWR revealed that, in the case of the foreign-continuum, the function with minor corrections is capable of reproducing available experimental data throughout the entire sub-THz frequency range. In the case of the self-continuum there is a significant difference between model and observations, which starts at about 0.4 THz and increases with frequency. The understanding of the mechanisms of continuum formation enabled an advancement in its physically based modeling, explicitly taking into account the spectral manifestations of pairwise interactions of molecules giving rise to bimolecular absorption. We have proposed a model of the atmospheric water vapor self-continuum in the region up to 1 THz in the form of a sum of contributions from the absorption by stable and metastable dimers and the absorption corresponding to unknown behavior of the far wings of the water monomer resonance lines. A plausible definition of all the types of molecular pairs contributing to the continuum is expected to allow individual refining of each component without recourse to reconsideration of the whole absorption model. Note that such flexibility is not characteristic of any presently used approach to the continuum modeling.

The comparative analysis of the proposed continuum model, the PWR98 and all the most known experimental data from the literature on the self-continuum of atmospheric water vapor has shown that, in the frequency range under consideration, the new continuum model fits the experimental data better than the model from the current PWR23 version. We have demonstrated that the empirical representation of the foreign-continuum component from PWR98 after minor modification agrees with all known experimental data (laboratory and field measurements using horizontal paths) within the limits of measurement

uncertainty. The proposed changes of the water vapor self- and foreign-continuum components in the PWR model may lead to systematic differences in brightness temperature calculations, reaching up to about 1 and 4.7 K, respectively in the sub-THz.

The proposed model should be still considered as semiempirical because the shape and amplitude of the continuum components are fitted to currently available experimental data. However, we demonstrated that the used approach already allows non-empirical simulation of the continuum in pure nitrogen and its mixture with Ar in broad spectral and temperature ranges, which opens up an opportunity for dry air continuum non-empirical modeling [79]. We look forward to extending the method to polar atmospheric species for the final solution of the long standing problem of atmospheric continuum.

Fortran codes for the proposed in this work models of atmospheric continuum components (including the non-empirical model of the dry air continuum developed on the basis of N_2-N_2 collision induced absorption simulation in [79] and efficiency factors to take into account N_2-O_2 and O_2-O_2 collisions from [80]) are in open access from the PyRTLib repository [23].

CRediT authorship contribution statement

M.Yu. Tretyakov: Writing – review & editing, Validation, Supervision, Project administration, Methodology, Conceptualization. **T.A. Galanina:** Writing – original draft, Visualization, Methodology, Formal analysis, Data curation. **A.O. Koroleva:** Visualization, Validation, Software, Formal analysis. **D.S. Makarov:** Visualization, Software, Formal analysis. **D.N. Chistikov:** Software, Investigation, Formal analysis. **A.A. Finenko:** Software, Investigation, Formal analysis. **A.A. Vigasin:** Writing – review & editing, Validation, Methodology, Conceptualization.

Declaration of competing interest

The authors declare that they have no known competing financial interests or personal relationships that could have appeared to influence the work reported in this paper.

Appendix. Water-related continuum modeling

The appendix collects formulas for water-related continuum modeling for practical applications.

Table A1
Physical quantities and their units.

Symbol Parameter	α Absorption	f Frequency	P Pressure	T Temperature	K_x Equilibrium constant
Units	cm^{-1}	GHz	mbar	K	atm^{-1}

Total continuum absorption:

$$\alpha_{cont}(f, P, T) = \alpha_{self}(f, P, T) + \alpha_{foreign}(f, P, T) \tag{A1}$$

1 Self-continuum modeling (Section 3 of the paper)

Water vapor self-continuum is considered as a sum of absorption of bound dimers $\alpha_{BD}(f, P, T)$, metastable dimers $\alpha_{MD}(f, P, T)$, and far line wings $\alpha_{FW}(f, P, T)$

Table A1, A2, A3

$$\alpha_{self}(f, P, T) = \alpha_{BD}(f, P, T) + \alpha_{MD}(f, P, T) + \alpha_{FW}(f, P, T) \tag{A2}$$

1.1 Bound dimer

$$\alpha_{BD}(f, P, T) = S_{BD}(f)\left(\frac{268}{T}\right)^{10} f^2 P^2 \tag{A3}$$

$$S_{BD}(f) = \left(\frac{a_0}{(a_1)^2 + (f - a_2)^2} + \frac{a_3}{(a_4)^2 + (f)^2} + a_5\right) \tag{A4}$$

Table A2

Parameters of bound dimer spectral function Eq. (A4).

Parameter	Value	Units
a_0	$5.5474 \bullet 10^{-8}$	$cm^{-1}\ GHz^{-1}mbar^{-2}$
a_1	434.75	GHz
a_2	219.45	GHz
a_3	$4.9264 \bullet 10^{-10}$	$cm^{-1}\ GHz^{-1}mbar^{-2}$
a_4	21.062	GHz
a_5	$1.344 \bullet 10^{-14}$	$cm^{-1}GHz^{-2}mbar^{-2}$

Table A3

Numerical coefficients for Eq. (A9).

b_0	$-7.804242 \bullet 10^6$	b_5	$3.017768 \bullet 10^{-6}$
b_1	$8.345651 \bullet 10^4$	b_6	$-2.518957 \bullet 10^{-9}$
b_2	$-4.212794 \bullet 10^2$	b_7	$1.350628 \bullet 10^{-12}$
b_3	1.242946	b_8	$-4.134191 \bullet 10^{-16}$
b_4	$-2.409822 \bullet 10^{-3}$	b_9	$5.530774 \bullet 10^{-20}$

1.2 Metastable dimer

$$\alpha_{MD}(f, P, T) = \left[0.3 \cdot S_{2mon}(f, T_0) \left(\frac{266}{T} \right)^{2.9} + 0.7 \cdot \frac{S_{BD}(f)}{K_{BD}(T)} \left(\frac{268}{T} \right)^{10} \right] K_{MD}(T) f^2 P^2 \tag{A5}$$

$$S_{2Mon}(f) = \frac{10^{-10}}{1013.25} (4.06 + 7.119 \cdot 10^{-3} f), \quad \frac{cm^{-1}}{GHz^2 mbar^2} \tag{A6}$$

$$K_{BD}(T) = 4.7856 \cdot 10^{-4} \cdot exp \left\{ \frac{1669.8}{T} - 5.10485 \cdot 10^{-3} T \right\}, \quad atm^{-1} \tag{A7}$$

$$K_{MD}(T) = -\frac{B(T)}{RT} - K_{BD}(T) + \frac{30.5}{RT}, atm^{-1} \tag{A8}$$

$R = 82.05746$ – molar gas constant in $cm^3 atm\ K^{-1}\ mol^{-1}$

$$B(T) = \left(\frac{100}{T} \right)^6 (b_0 + b_1 \cdot T + b_2 \cdot T^2 + b_3 \cdot T^3 + b_4 \cdot T^4 + b_5 \cdot T^5 + b_6 \cdot T^6 + b_7 \cdot T^7 + + b_8 \cdot T^8 + b_9 \cdot T^9) [cm^3 / molecule] \tag{A9}$$

1.3 Far wings

$$\alpha_{FW}(f, P, T) = 7 \cdot 10^{-15} \cdot f^{2.2} P^2 \left(\frac{296}{T} \right)^{1.5}, cm^{-1} \tag{A10}$$

2 Foreign-continuum modeling (Sect. 4 of the paper)

$$\alpha_{foreign}(f, P_{air}, P_{H_2O}, T) = 7.1 \cdot 10^{-15} P_{air} P_{H_2O} f^{1.96} \left(\frac{300}{T} \right)^{4.4}, cm^{-1} \tag{A11}$$

Data availability

Data will be made available on request.

References

[1] Ptashnik IV. Evidence for the contribution of water dimers to the near-IR water vapour self-continuum. J Quant Spectrosc Radiat Transfer 2008;109:831–52.

[2] Shine KP, Ptashnik IV, Rädel G. The water vapour continuum: brief history and recent developments. Surv Geophys 2012;33(3–4):535–55.

[3] Tretyakov MYu, Koshelev MA, Serov EA, Parshin VV, Odintsova TA, Bubnov GM. Water dimer and the atmospheric continuum. Physics – Uspekhi, V. 2014;57(11):1083–98.

[4] Ptashnik IV. Water vapour continuum absorption: short prehistory and current status. Optika Atmosfery i Okeana 2015;28(5):443–59 [in Russian].

[5] Frommhold L. Collision induced absorption in gases. Cambridge University Press; 2006.

[6] Vigasin AA. Bimolecular absorption in atmospheric gases. In: Camy-Peyret C, Vigasin AA, editors. Weakly Interacting Molecular Pairs: Unconventional Absorbers of Radiation in the Atmosphere. Dordrecht: Kluwer; 2003. p. 23–47.

[7] Tretyakov MYu. High accuracy resonator spectroscopy of atmospheric gases at millimetre and submillimetre waves. Cambridge Scholars Publishing; 2021.

[8] Ptashnik IV, Shine KP, Vigasin AA. Water vapour self-continuum and water dimers: 1. Analysis of recent work. J Quant Spectrosc Radiat Transf 2011;112:1286–303.

[9] Odintsova TA, Koroleva AO, Simonova AA, Campargue A, Tretyakov MYu. The atmospheric continuum in the "terahertz gap" region (15–700 cm⁻¹): review of experiments at SOLEIL synchrotron and modeling. J Mol Spectrosc 2022;386: 111603.

[10] Simonova AA, Ptashnik IV, Shine KP. Semi-empirical water dimer model of the water vapour self-continuum within the IR absorption bands. J Quant Spectrosc Radiat Transf 2024;329:109198. https://doi.org/10.1016/j.jqsrt.2024.109198.

[11] Mlawer EJ, Cady-Pereira KE, Mascio J, Gordon IE. The inclusion of the MT_CKD water vapor continuum model in the HITRAN molecular spectroscopic database. J Quant Spectrosc Radiat Transf 2023;306:108645.

[12] Ptashnik IV, Klimeshina TE, Solodov AA, Vigasin AA. Spectral composition of the water vapour self-continuum absorption within 2.7 and 6.25 μm bands. J Quant Spectrosc Radiat Transf 2019;228:97–105.

[13] Galanina TA, Koroleva AO, Simonova AA, Campargue A, Tretyakov MYu. The water vapor self-continuum in the "terahertz gap" region (15–700 cm⁻¹): experiment versus MT_CKD-3.5 model. J Mol Spectrosc 2022;389:111691.

[14] Koroleva AO, Kassi S, Campargue A. The water vapor self-continuum absorption at room temperature in the 1.25 μm window. J Quant Spectrosc Radiat Transf 2022;286: 108206.

[15] Brogniez H, English S, Mahfouf J-F, Behrendt A, Berg W, Boukabara S, Buehler SA, Chambon P, Gambacorta A, Geer A, Ingram W, Kursinski ER, Matricardi M, Odintsova TA, Payne VH, Thorne PW, Tretyakov MYu, Wang J. A review of sources of systematic errors and uncertainties in observations and simulations at 183 GHz. Atmos Meas Tech 2016;9:2207–21.

[16] Cimini D, Rosenkranz PW, Tretyakov MYu, Koshelev MA, Romano F. Uncertainty of atmospheric microwave absorption model: impact on ground-based radiometer simulations and retrievals. Atmos Chem Phys 2018;18:15231–59.

[17] E. Turner, S. Fox, V. Mattioli, D. Cimini, Literature review on microwave and Sub-millimetre spectroscopy for MetOp second generation. Technical Report (NWPSAF-MO-TR-039) 1–101, 2022.

[18] Gallucci D, Cimini D, Turner E, Fox S, Rosenkranz PW, Tretyakov MYu, Mattioli V, Larosa S, Romano F. Uncertainty in simulated brightness temperature due to sensitivity to atmospheric gas spectroscopic parameters from the centimeter- to submillimeter-wave range. Atmos Chem Phys 2024;24:7283–308.

[19] Serov EA, Odintsova TA, Tretyakov MYu, Semenov VE. On the origin of the water vapor continuum absorption within rotational and fundamental vibrational bands. J Quant Spectrosc Rad Transf 2017;193:1–12.

[20] Gambacorta A, Piepmeier J, Stephen M, Santanello J, Blaisdell J, Moradi I, McCarty W, Rosenberg R, Kotsakis A, Gambini F, Mohammed P, Kroodsma R, MacKinnon J, Adams I, Racette P. Advancing atmospheric thermodynamic sounding from space using Hyperspectral microwave measurements. IEEE J Sel Top Appl Earth Observat Remote Sens 2023;16:5204–18.

[21] Liebe HJ, Gimmestad GG. Calculation of clear air EHF refractivity. Radio Sci 1978: 245–51. V. 13. N. 2.

[22] Rosenkranz PW. Line-by-line microwave radiative transfer (non-scattering). Remote Sens. Code Lib 2017. https://doi.org/10.21982/M81013.

[23] http://cetemps.aquila.infn.it/mwrnet/lblmrt_ns.html (Dec. 4, 2024).

[24] Liebe HJ. Modeling attenuation and phase of radio waves in air at frequencies below 1000 GHz. Radio Sci 1981;16(6):1183–99.

[25] Liebe HJ. An atmospheric millimeter-wave propagation model. NITA report 1983: 83–137.

[26] Bauer A, Godon M, Kheddar M, Hartmann J-M. Temperature and perturber dependences of water vapor line-broadening. Experiments at 183 GHz; calculations below 1000 GHz. J Quant Spectrosc Radiat Transf 1989;41(1):49–54.

[27] H.J. Liebe, D.H. Layton, Millimeter-wave properties of the atmosphere: laboratory studies and propagation modeling, NTIA report, 87–224, 1987.

[28] Gordon IE, Rothman LS, Hargreaves RJ, Hashemi R, Karlovets EV, Skinner FM, Conway EK, Hill C, Kochanov RV, Tan Y, Wcisło P, Finenko AA, Nelson K, Bernath PF, Birk M, Boudon V, Campargue A, Chance KV, Coustenis A, Drouin BJ, Flaud JM, Gamache RR, Hodges JT, Jacquemart D, Mlawer EJ, Nikitin AV, Perevalov VI, Rotger M, Tennyson J, Toon GC, Tran H, Tyuterev VG, Adkins EM, Baker A, Barbe A, Canè E, Császár AG, Dudaryonok A, Egorov O, Fleisher AJ, Fleurbaey H, Foltynowicz A, Furtenbacher T, Harrison JJ, Hartmann J-M, Horneman VM, Huang X, Karman T, Karns J, Kassi S, Kleiner I, Kofman V, Kwabia-Tchana F, Lavrentieva NN, Lee TJ, Long DA, Lukashevskaya AA, Lyulin OM, Makhnev VY, Matt W, Massie ST, Melosso M, Mikhailenko SN, Mondelain D, Müller HSP, Naumenko OV, Perrin A, Polyansky OL, Raddaoui E, Raston PL, Reed ZD, Rey M, Richard C, Tóbiás R, Sadiek I, Schwenke DW, Starikova E, Sung K, Tamassia F, Tashkun SA, Vander Auwera J, Vasilenko IA, Vigasin AA, Villanueva GL, Vispoel B, Wagner G, Yachmenev A, Yurchenko SN. The HITRAN2020 molecular spectroscopic database. J Quant Spectrosc Radiat Transf 2022;277:107949.

[29] Clough SA, Kneizys FX, Davies RW. Line shape and the water vapor continuum. Atmos Res 1989;23:229–41.

[30] Rosenkranz PW. Water vapor microwave continuum absorption: a comparison of measurements and models. Radio Sci 1998;33(4):919–28.

[31] Koshelev MA, Serov EA, Parshin VV, Tretyakov MYu. Millimeter wave continuum absorption in moist nitrogen at temperatures 261–328 K. J Quant Spectr Radiat Transf 2011;112:2704–12.

[32] Turner DD, Cadeddu MP. Modifications to the water vapor continuum in the microwave suggested by ground-based 150-GHz observations. IEEE Trans Geosci Remote Sens 2009;47(10):3326–37.

[33] Payne VH, Mlawer EJ, Cady-Pereira KE, Moncet J-L. Water vapor continuum absorption in the microwave. IEEE Trans Geosci Remote Sens 2011;49(6): 2194–208.

[34] Wentz FJ, Meissner T. Atmospheric absorption model for dry air and water vapor at microwave frequencies below 100 GHz derived from spaceborne radiometer observations. Radio Sci 2016;51:381–91.

[35] Odintsova TA, Tretyakov MYu, Pirali O, Roy P. Water vapor continuum in the range of rotational spectrum of H₂O molecule: new experimental data and their comparative analysis. J Quant Spectrosc Rad Transf 2017;187:116–23.

[36] Odintsova TA, Tretyakov MYu, Zibarova AO, O.Pirali PRoy, Campargue A. Far-infrared self-continuum absorption of H₂¹⁶O and H₂¹⁸O (15–500 cm⁻¹). J Quant Spectrosc Rad Transf 2019;227:190–200.

[37] Burch D. Continuum absorption by atmospheric H₂O. Proc. SPIE 1981;277:28–39.

[38] Kuhn T, Bauer A, Godon M, Buehler S, Kuenzi K. Water vapor continuum: absorption measurements at 350 GHz and model calculations. J Quant Spectrosc Radiat Transf 2002;74:545–62.

[39] Katkov VYu, Sverdlov BA, Furashov NI. Experimental estimates of the value and temperature dependence of the air-humidity quadratic component of the atmospheric water-vapor absorption coefficient in the frequency band of 140-410 GHz. Radiophys Quant Electron 1995;38(12):835–44.

[40] Podobedov VB, Plusquellic DF, Siegrist KE, Fraser GT, Ma Q, Tipping RH. New measurements of the water vapor continuum in the region from 0.3 to 2.7 THz. J Quant Spectrosc Radiat Transf 2008;109:458–67.

[41] Storgyn DE, Hirschfelder JO. Contribution of bound, metastable, and free molecules to the second virial coefficient and some properties of double molecules. J Chem Phys 1959;31:1531–45.

[42] Vigasin AA. Bound, metastable and free states of bimolecular complexes. Infrared Phys 1991;32:461–70.

[43] Vigasin AA. Water vapor continuum: whether collision-induced absorption is involved? J Quant Spectrosc Radiat Transf 2014;148:58–64.

[44] Leforestier C, Tipping RH, Ma Q. Temperature dependences of mechanisms responsible for the water-vapor continuum absorption. II. Dimers and collision-induced absorption. J Chem Phys 2010;132:164302.

[45] Tretyakov MYu, Sysoev AA, Odintsova TA, Kyuberis AA. Collision-Induced dipole moment and millimeter and submillimeter continuum absorption in water vapor. Radiophys Quantum Electron 2015;58(4):262–76.

[46] Townes CH, Schawlow A. Microwave spectroscopy. N. Y.: McGrow-Hill; 1955.

[47] Wagner W, Pruss A. The IAPWS formulation 1995 for the thermodynamic properties of ordinary water substance for general and scientific use. J Phys Chem Ref Data 2002;31(2):387–535.

[48] Leforestier C. Water dimer equilibrium constant calculation: a quantum formulation including metastable states. J Chem Phys 2014;140:074106.

[49] Tretyakov MYu, Serov EA, Odintsova TA. Equilibrium thermodynamic state of water vapor and the collisional interaction of molecules. Radiophys Quantum Electron 2012;54(10):700–16.

[50] Galanina TA, Koroleva AO, Amerkhanov IS, Serov EA, Koshelev MA, Tretyakov MYu, Chistikov DN, Finenko AA, Vigasin AA. On the nature of sub-THz continuum absorption in CO₂ gas, its mixture with Ar, and in pure water vapor. Phys Chem Chem Phys 2024;26:15032–43. https://doi.org/10.1039/D4CP00240G.

[51] Scribano Y, Goldman N, Saykally RJ, Leforestier C. Water dimers in the atmosphere. III. Equilibrium constant from a flexible potential. J Phys Chem A 2006;110:5411–9.

[52] Rocher-Casterline BE, Ch'ng LC, Mollner AK, Reisler H. Determination of the bond dissociation energy (D₀) of the water dimer, (H₂O)₂, by velocity map imaging. J Chem Phys 2011;134:211101.

[53] Scribano Y, Leforestier C. Contribution of water dimer absorption to the millimeter and far infrared atmospheric water continuum. J Chem Phys 2007;126:234301.

[54] Tretyakov MYu, Serov EA, Koshelev MA, Parshin VV, Krupnov AF. Water Dimer rotationally resolved millimeter-wave spectrum observation at room temperature. Phys Rev Lett 2013;110:093001.

[55] Serov EA, Koshelev MA, Odintsova TA, Parshin VV, Tretyakov MYu. Rotationally resolved water dimer spectra in atmospheric air and pure water vapour in the 188 - 258 GHz range. Phys Chem Chem Phys 2014;16(47):26221–33.

[56] Koshelev MA, Leonov II, Serov EA, Chernova AI, Balashov AA, Bubnov GM, Andriyanov AF, Shkaev AP, Parshin VV, Krupnov AF, Tretyakov MYu. New frontiers of modern resonator spectroscopy. IEEE Trans Terahertz Sci Technol 2018;8(6):773–83.

[57] Vigasin A. On the possibility to quantify contributions from true bound and metastable pairs to infrared absorption in pressurised water vapour. Mol Phys 2010;108:2309–13.

[58] Odintsova TA, Tretyakov MYu. Evidence of true bound and metastable dimers and trimers presence in high temperature water spectra. J Quant Spectrosc Rad Trans 2013;120:134–7.

[59] Van Wleck JH, Huber DL. Absorption, emission, and linebreadths:a semihistorical perspective. Rev Mod Phys 1977;49(4):939–59.

[60] Hartmann J-M, Boulet C, Robert D. Collisional effects on molecular spectra. Elsevier; 2021.

[61] Odintsova TA, Tretyakov MYu, Simonova AA, Ptashnik IV, Pirali O, Campargue A. Measurement and temperature dependence of the water vapor self-continuum between 70 and 700 cm⁻¹. J Mol Struct 2020;1210:128046.

[62] https://github.com/AER-RC/MT_CKD_H2O/releases/tag/4.3 (Dec. 4, 2024).

[63] Bauer A, Godon M, Carlier J, Ma Q, Tipping RH. Absorption by H₂O and H₂O-N₂ mixtures at 153 GHz. J Quant Spectrosc Radiat Transf 1993;50:463–75.

[64] Bauer A, Godon M, Carlier J, Ma Q. Water vapor absorption in the atmospheric window at 239 GHz. J Quant Spectrosc Radiat Transf 1995;53:411–23.

[65] Godon M, Carlier J, Bauer A. Laboratory studies of water vapor absorption in the atmospheric window at 213 GHz. J Quant Spectrosc Radiat Transf 1992;47: 275–85.

[66] Podobedov VB, Plusquellic DF, Siegrist KM, Fraser GT, Ma Q, Tipping RH. Continuum and magnetic dipole absorption of the water vapor – oxygen mixtures from 0.3 to 3.6 THz. J Mol Spectrosc 2008;251:203–9.

[67] Pardo JR, Serabyn E, Cernicharo J. Submillimeter atmospheric transmission measurements on Mauna Kea during extremely dry El Nino conditions: implications for broadband opacity contributions. J Quant Spectrosc Rad Transf 2001;68:419–33.

[68] Ivanov SV. Quasi-bound complexes in collisions of different linear molecules: classical trajectory study of their manifestations in rotational relaxation and spectral line broadening. J Quant Spectrosc Radiat Transf 2016;177:269–82.

[69] Chistikov DN, Finenko AA, Kalugina YN, Lokshtanov SE, Petrov SV, Vigasin AA. Simulation of collision-induced absorption spectra based on classical trajectories and ab initio potential and induced dipole surfaces. II. CO_2–Ar rototranslational band including true dimer contribution. J Chem Phys 2021;155:064301. https://doi.org/10.1063/5.0060779.

[70] Odintsova TA, Serov EA, Balashov AA, Koshelev MA, Koroleva AO, Simonova AA, Tretyakov MYu, Filippov NN, Chistikov DN, Finenko AA, Lokshtanov SE, Petrov SV, Vigasin AA. CO_2–CO_2 and CO_2–Ar continua at millimeter wavelengths. J Quant Spectrosc Rad Transf 2021;258:107400.

[71] Leforestier C, Szalewicz K, van der Avoird A. Spectra of water dimer from a new ab initio potential with flexible monomers. J Chem Phys 2012;137:014305. https://doi.org/10.1063/1.4722338.

[72] Tretyakov MYu, Serov EA, Odintsova TA. Equilibrium thermodynamic state of water vapor and the collisional interaction of molecules. Radiophys Quantum Electron 2012;54(10):700–16.

[73] Leforestier C. Water dimer equilibrium constant calculation: a quantum formulation including metastable states. J Chem Phys 2014;140:074106.

[74] Slocum DM, Slingerland EJ, Giles RH, Goyette TM. Atmospheric absorption of terahertz radiation and water vapor continuum effects. J Quant Spectrosc Radiat Transf 2013;127:49–63.

[75] Vigasin AA. Mass-action law for highly excited dimers. Chem Phys Lett 1998;290: 495–501.

[76] Vigasin AA. Water vapor continuous absorption in various mixtures: possible role of weakly bound complexes. J Quant Spectrosc Radiat Transf 2000;64:25–40.

[77] Kjaergaard HG, Low GR, Robinson TW, Howard DL. Calculated OH-stretching vibrational transitions in the water-nitrogen and water-oxygen complexes. J Phys Chem A. 2002;106:8955–62.

[78] Larosa S, Cimini D, Galucci D, Nilo ST, Romano F. PyRTlib: an educational Python-based library for non-scattering atmospheric microwave Radiative Transfer computations. Geosci Model Dev 2024;17(5):2053–76. https://doi.org/10.5194/gmd-17-2053-2024.

[79] Serov EA, Galanina TA, Koroleva AO, Makarov DS, Amerkhanov IS, Koshelev MA, Tretyakov MYu, Chistikov DN, Finenko AA, Vigasin AA. Continuum absorption in pure N_2 gas and in its mixture with Ar. J Quant Spectrosc Radiat Transf 2024;328: 109172.

[80] Boissoles J, Boulet C, Tipping RH, Brown A, Ma Q. Theoretical calculation of the translation-rotation collision-induced absorption in N_2-N_2, O_2-O_2, and N_2-O_2 pairs. J Quant Spectrosc Radiat Transf 2003;82:505–16.

[81] Finenko AA, Serov EA, Koroleva AO, Makarov DS, Koshelev MA, Chistikov DN, Tretyakov MYu, Vigasin AA. Physical background of dry atmospheric continuum modeling from microwave measurements and N_2-N_2 collisional scattering simulations. In: 2024 IEEE 9th All-Russian Microwave Conference (RMC-2024). Conference Proceedings; 2024. Moscow, Russia, Accepted for publication in IEEE Xplore Digital Library Conference number 62880.